Different Bonding Modes of the C_7 Ring on Iridium Clusters. Synthesis, Electrochemistry, and Solid State Structure of $[Ir_6(CO)_{13}(\mu_3\text{-}\eta^2\text{:}\eta^2\text{:}\eta^2\text{-}C_7H_8)]$, $[Ir_6(CO)_{12}(\mu_3\text{-}\eta^2\text{:}\eta^3\text{:}\eta^2\text{-}C_7H_7)]^-$, and $[Ir_6(CO)_{12}(\mu_3\text{-}\eta^2\text{:}\eta^2\text{:}\eta^2\text{-}C_7H_8)]^{2-}$

Roberto Della Pergola,*[,†] Anna Bianchi,[‡] Fabrizia Fabrizi de Biani,[§] Luigi Garlaschelli,[‡] Mario Manassero,*[,⊥] Mirella Sansoni,[⊥] Donatella Strumolo,[‡] and Piero Zanello[§]

Dipartimento di Scienze dell'Ambiente e del Territorio, Università di Milano Bicocca, Piazza della Scienza 1, 20126 Milano, Italy, Dipartimento di Chimica Inorganica, Metallorganica ed Analitica, Università di Milano, Via G. Venezian 21, 20133 Milano, Italy, Dipartimento di Chimica dell'Università, Via A. Moro -53100 Siena, Italy, and Dipartimento di Chimica Strutturale e Stereochimica Inorganica, Università di Milano, Via G. Venezian 21-20133 Milano, Italy

Received June 4, 2002

The cluster $[Ir_6(CO)_{13}(C_7H_8)]$ (**1**) was synthesized from $[Ir_6(CO)_{16}]$ and excess cycloheptatriene in refluxing toluene. In the solid state, the six iridium atoms define an octahedral metal cage, and one face is capped by the $\mu_3\text{-}\eta^2\text{:}\eta^2\text{:}\eta^2\text{-}C_7H_8$ ligand, which is a six-electrondonor, through the three C═C double bonds. Reaction of **1** with Na_2CO_3 in THF yields $[Ir_6(CO)_{12}(C_7H_7)]^-$ (**2**). In this octahedral anion, the cycloheptatrienyl ring is almost planar and is coordinated to a triangular face in the $\mu_3\text{-}\eta^2\text{:}\eta^3\text{:}\eta^2$-fashion. Reaction of **1** or **2** with NaOH in THF yields $[Ir_6(CO)_{12}(C_7H_8)]^{2-}$ (**3**), in which a $\mu_3\text{-}\eta^2\text{:}\eta^2\text{:}\eta^2\text{-}C_7H_8$ is also present. The ^1H NMR spectra of **1** and **3** show five signals, which were assigned to the nonequivalent hydrogen atoms by bidimensional experiments. The spectrum of **2** shows a singlet, even at low temperature, in agreement with a highly fluxional ligand. The interconversions of **1** to the anions **2** and **3**, respectively, have been followed by electrochemical investigations. The neutral $[Ir_6(CO)_{13}(C_7H_8)]$ proves to undergo a two-electron reduction, which, being accompanied by decarbonylation, affords the dianion $[Ir_6(CO)_{12}(C_7H_8)]^{2-}$. In turn, the latter undergoes a two-electron oxidation, which followed by deprotonation affords the monoanion $[Ir_6(CO)_{12}(C_7H_7)]^-$.

Several clusters bearing carbocyclic unsaturated ring have been isolated and described in the past few years.[1] The interest in this type of compound has been concentrated, so far, in their synthesis, and their supramolecular solid state arrangements. The steric relevance of the organic ligand and the presence of functional groups induce different packing of the clusters, which is the basis of so-called organometallic crystal engineering. The most relevant studies have been dedicated to hexanuclear derivatives of ruthenium, substituted by arene ligands.[2]

The cycloheptratriene is a widely employed ligand in organometallic chemistry: mononuclear and cluster compounds, containing such a ring, are well documented in the literature. When supported by a cluster, the C_7 rings can bind one, two, or three metal atoms. Relevant examples of these different bonding modes are (i) $[Ru_6C(CO)_{11}(C_7H_9)(C_7H_7)]$[3] and $[Co_4(CO)_6(C_7H_9)(C_7H_7)]$,[4] where the $\eta^5\text{-}C_7H_9$ and the $\mu_3\text{-}\eta^7\text{-}C_7H_7$ arrangements are displayed in the same molecule, (ii) $[Ru_4(CO)_7(C_7H_7)_2]$, which contains edge-bridging $\mu_2\text{-}\eta^3\text{:}\eta^4$ units,[5] and (iii) $[Ru_6C(CO)_{14}(C_7H_8)]$, where a facial $\mu_3\text{-}\eta^2\text{:}\eta^2\text{:}\eta^2$ is present.[3] Upon coordination to several metal atoms, the reactivity of the ring is modified, and the hapticity of the ligand can be changed either by a ring contraction,[3] by reductive coupling,[6] or by a ligand-to-ligand hydrogen trans-

* Corresponding authors. (R.D.P.) Fax: +39-0264482890. E-mail: roberto.dellapergola@unimib.it. (M.M.) E-mail: m.manassero@csmtbo.mi.cnr.it.
† Dipartimento di Scienze dell'Ambiente e del Territorio, Università di Milano Bicocca.
‡ Dipartimento di Chimica Inorganica, Metallorganica ed Analitica, Università di Milano.
§ Dipartimento di Chimica dell'Università di Siena.
⊥ Dipartimento di Chimica Strutturale e Stereochimica Inorganica, Università di Milano.

(1) (a) Johnson, B. F. G.; Dyson, P. J.; Martin, C. M. *J. Chem. Soc., Dalton Trans.* **1996**, 2395. (b) Deeming, A. J. In *Metal Clusters in Chemistry*; Braunstein, P., Oro, L. A., Raithby, P. R., Eds.; Wiley-VCH: New York, 1999; p 235. (c) Raithby, P. R.; Shields, G. P. *Polyhedron* **1998**, *17*, 2829.
(2) (a) Dyson, P. J.; Johnson, B. F. G.; Reed, D.; Braga, D.; Grepioni, F.; Parisini, E. *J. Chem. Soc., Dalton Trans.* **1993**, 2817. (b) Braga, D.; Dyson, P. J.; Grepioni, F.; Johnson, B. F. G. *Chem. Rev.* **1994**, *94*, 1585.
(3) Braga, D.; Grepioni, F.; Scaccianoce, L.; Johnson, B. F. G. *J. Chem. Soc., Dalton Trans.* **1998**, 1321.
(4) Wadepohl, H.; Gebert, S.; Pritzkow, H.; Grepioni, F.; Braga, D. *Chem. Eur. J.* **1998**, *4*, 279.
(5) Braga, D.; Dyson, P. J.; Grepioni, F.; Johnson, B. F. G.; Martin, C. M.; Scaccianoce, L.; Steiner, A. *J. Chem. Soc., Chem. Commun.* **1997**, 1259.
(6) Wadepohl, H.; Gebert, S.; Pritzkow, H.; Osella, D.; Nervi, C.; Fiedler, J. *Eur. J. Inorg. Chem.* **2000**, 1833.

10.1021/om0204437 CCC: $22.00
Publication on Web 11/02/2002

fer.[3,4] Although the organic chemistry of the C_5 ring was much more explored than that of the metal-coordinated cycloheptatriene,[7] a few examples of clusters containing derivatized C_7H_7R ligands have been described.[6,8]

Stable metallic cages and functionalized organic ligands can be combined in the same molecule, opening the way to organometallic polymers or to metal-based molecular devices.[9] Face-bridging carbocycles are particularly suited for this purpose, since they reinforce the metal−metal bonds of the atoms to which they are bonded, increasing the stability of the cluster.[10] Resistance toward fragmentation and multiple coordinating ability make these species good candidates for cluster catalysis.[11] These studies were concentrated, so far, to cobalt and ruthenium compounds.

We report here the synthesis of $[Ir_6(CO)_{13}(C_7H_8)]$ and its reactivity toward reagents of increased basicity. When the cluster is stepwise reduced to $[Ir_6(CO)_{12}(C_7H_7)]^-$ and $[Ir_6(CO)_{12}(C_7H_8)]^{2-}$, its 86 valence electrons are kept constant by modifying the hapticity of the C_7 ring.

Only a few large iridium clusters, substituted by hydrocarbons, have been isolated so far: they include the alkyne-substituted $[Ir_6(CO)_{14}(\mu_3\text{-}\eta^2\text{-PhCCPh})]$, $[Ir_6(CO)_{12}(\mu_3\text{-}\eta^2\text{-PhCCPh})_2]$,[12] and the polysubstituted $[Ir_7(CO)_{12}(C_8H_{12})(C_8H_{11})(C_8H_{10})]$, showing stages of cyclooctadiene dehydrogenation.[13]

Results

(1) Syntheses. (1a) Synthesis of $[Ir_6(CO)_{13}(C_7H_8)]$. The neutral derivative **1** was obtained by carbonyl substitution, suspending $Ir_6(CO)_{16}$ (**4**) and a large excess of C_7H_8 in toluene, and heating the mixture to reflux for about 8 h. The unsubstituted reactant **4** is totally insoluble in toluene, and the product **1** is moderately soluble. Therefore, the formation of the new product is confirmed by the darkening of the solution. The reaction times decrease if the starting material is freshly prepared, in agreement with aging of solid $Ir_6(CO)_{16}$. When the obtained solution is cooled slowly to room temperature, the product precipitates partially, sometimes in the form of well-shaped crystals of **1**·CH_3Ph, which have been used for X-ray analysis.

(1b) Synthesis of $[Ir_6(CO)_{12}(C_7H_7)]^-$. The monoanionic derivative **2** can be prepared from **1** and sodium carbonate in THF at room temperature. The reaction is selective, and IR monitoring shows complete conversion after about 4 h.

Although we do not have any experimental evidence, we suggest that the mechanism does not involve a deprotonation of the C_7H_8 ligand, but rather the attack of a base on a carbonyl of the cluster, with the formation of a metal hydride, followed by intramolecular oxidative addition of the unique methylene group and concomitant elimination of hydrogen. The product can be recovered as a tetraalkylammonium salt, after metathesis with the corresponding halide in methanol. Yields at this stage are higher than 70%, but after crystallization from thf/hexane they are lowered to about 60−50%.

(1c) Synthesis of $[Ir_6(CO)_{12}(C_7H_8)]^{2-}$. To speed up the slow reduction of **1** to **2**, we tested a homogeneous reaction, by adding a few drops of NEt_4OH in MeOH to a THF solution of **1**. Under these conditions, instead of the expected monoanion, a different, more reduced product, **3**, was selectively formed. Methanolic NaOH afforded the same anion **3**, and this reagent was usually used, since the sodium salt Na_2**3** can be converted in any convenient salt, by metathesis with ammonium or phosphonium cation: the salt $[NEt_4]_2$**3** was used for elemental analysis, $[NMe_3CH_2Ph]_2$**3** for X-ray, and $[PPh_4]_2$**3** for the ^1H NMR, since the signals of the C_7H_8 ligand and the $[PPh_4]^+$ cation are very distinct.

The reaction of **1** and hydroxide ions is quite fast, but requires an excess of NaOH to ensure quantitative formation of **3**. Otherwise, mixtures of products are formed. For this reason, we could not identify the intermediate products of the reaction and could not establish if NaOH and Na_2CO_3 act by different mechanisms. To see if $[Ir_6(CO)_{12}(C_7H_7)]^-$ has a role in this transformation, the monoanion **2** was also allowed to react with NaOH, and the conversion to $[Ir_6(CO)_{12}(C_7H_8)]^{2-}$ was verified. This is formally the addition of a hydride to the cycloheptatrienyl ligand and cannot be classified among the classical organometallic reactions. As an attempt to explain the mechanism, we suggest that the monoanion **2** is reduced with base to an unstable hydride, $[Ir_6(CO)_{11}(C_7H_7)H]^{2-}$, which can scavenge traces of CO from the solution and eliminate the $-CH_2-$ unit, through formation of a new C−H bond. Accordingly, the reduction of **2** to **3** can be performed with $NaBH_4$ in THF.

However, these reactions show that the cluster can assist the addition of nucleophiles to the cycloheptatrienyl ligand, and we hope to find the way to functionalize the carbocycle. Disappointingly, when the reactivity of **2** with iodide or methoxide was explored, discouraging results have been obtained.

The dianion **3** reacts with acids or $[Cp_2Fe]PF_6$, but **2** is only a minor product. These experiments provided chemical evidence that the interconversions of **1**, **2**, and **3** involve complicated mechanisms, prompting the electrochemical investigations.

(2) Electrochemistry. To ascertain the redox paths that govern the electron transfer passages from the neutral $[Ir_6(CO)_{13}(\eta^6\text{-}C_7H_8)]$ to the anions $[Ir_6(CO)_{12}(\eta^7\text{-}C_7H_7)]^-$ and $[Ir_6(CO)_{12}(\eta^6\text{-}C_7H_8)]^{2-}$, respectively, an electrochemical investigation has been carried out. In this connection, Figure 1 shows the voltammetric fingerprint of the three original derivatives in acetonitrile solution.

As illustrated in Figure 1a, $[Ir_6(CO)_{13}(\eta^6\text{-}C_7H_8)]$ undergoes either a reduction (peak A; $E_p = -0.65$ V) or an oxidation (peak B; $E_p = +0.93$ V), both of which possess features of chemical irreversibility (no well-shaped, directly associated return peak has been detected even at 5 V s^{-1}). Controlled potential coulometry in correspondence with the cathodic process ($E_w = -1.0$ V) consumes two electrons per molecule. In agreement with the cyclic voltammetric profile, the resulting solu-

(7) Elschenbroich, C; Salzer, A. *Organometallics, a Coincise Introduction*; VCH: Weinheim, 1989; pp 328−331.
(8) Ansell, G. B.; Bradley, J. S. *Acta Crystallogr. B* **1980**, *36*, 1930.
(9) (a) Schwab, P. F. H.; Levin, M. D.; Michl, J. *Chem. Rev.* **1999**, *99*, 474. (b) Johnson, B. F. G.; Sanderson, K. M.; Shepard, D. S.; Ozkaya, D.; Zhou, W.; Ahmed, H.; Thomas, M. D. R.; Gladden, L.; Mantle, M. *J. Chem. Soc., Chem. Commun.* **2000**, 1317.
(10) Wadepohl, H. *Coord. Chem. Rew.* **1999**, *185−186*, 551.
(11) Nagashima, H. *Monatsh. Chem.* **2000**, *131*, 12255.
(12) Ceriotti, A.; Della Pergola, R.; Demartin, F.; Garlaschelli, G.; Manassero, M.; Masciocchi, N. *Organometallics* **1992**, *11*, 756.
(13) Pierpont, C. G. *Inorg. Chem.* **1979**, *18*, 2972.

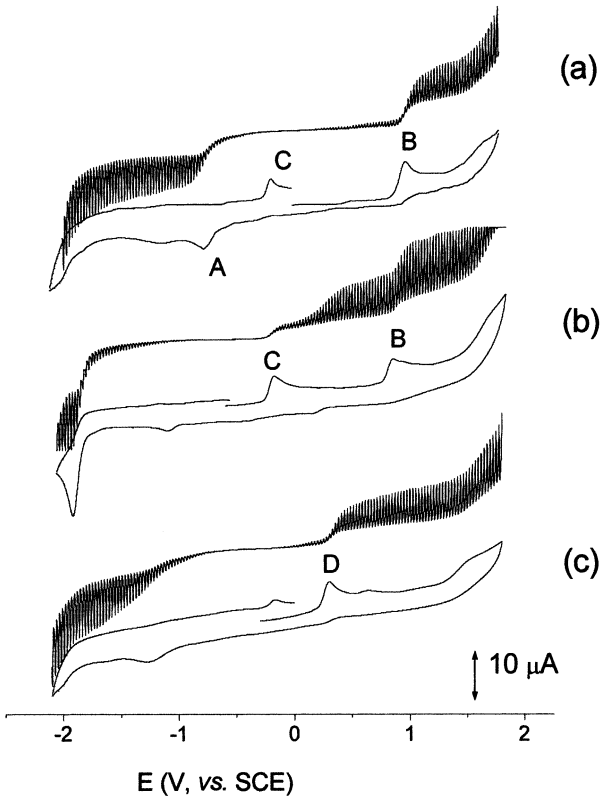

Figure 1. Hydrodynamic (top) and cyclic (bottom) voltammetric patterns exhibited at a platinum electrode by (a) $[Ir_6(CO)_{13}(\eta^6\text{-}C_7H_8)]$ (0.8×10^{-3} mol dm^{-3}); (b) $[Ir_6(CO)_{12}(\eta^6\text{-}C_7H_8)]^{2-}$ (1.1×10^{-3} mol dm^{-3}); (c) $[Ir_6(CO)_{12}(\eta^7\text{-}C_7H_7)]^{-}$ (1.3×10^{-3} mol dm^{-3}). MeCN solution containing $[NEt_4](PF_6)$ (0.1 mol dm^{-3}) as supporting electrolyte. Scan rates: (top) 0.02 V s^{-1}; (bottom) 0.2 V s^{-1}.

tion exhibits a first irreversible oxidation (peak C; $E_p = -0.20$ V) together with the above-mentioned oxidation process at higher potential values. As can be deduced from Figure 1b, such a voltammetric pattern arising from exhaustive two-electron reduction of **1** is quite coincident with that of the dianion **3**, thus indicating that the addition of two electrons to the neutral species to generate $[Ir_6(CO)_{12}(\eta^6\text{-}C_7H_8)]^{2-}$ is simply accompanied by decarbonylation (which accounts for the irreversibility of the process). Incidentally, the cathodic process present at about −1.9 V has to be ascribed to the reduction of the phosphonium countercation.

Figure 1c in turn shows that the monoanion $[Ir_6(CO)_{12}(\eta^7\text{-}C_7H_7)]^{-}$ exhibits a main oxidation process in correspondence with peak D ($E_p = +0.3$ V). This being stated, we proved that controlled potential coulometry ($E_w = 0.0$ V) in correspondence with the first oxidation process of the dianion **3** (namely, peak C) consumes two electrons per molecule and generates a voltammetric profile in which peak D appears and becomes predominant (even if a consistent appearance of peak B also occurs).[14] Really, such a conversion can be already observed in the hydrodynamic low scan oxidation profile pertinent to $[Ir_6(CO)_{12}(\eta^6\text{-}C_7H_8)]^{2-}$ under the form of a wave at about +0.3 V (Figure 1b).

In summary, we showed that **2** is not an intermediate of the electrochemical reduction **1** → **3**. Consistently, in the voltammetric profiles, there is no trace of the **1** → **2** and **2** → **3** reductions, both involving hydrogen transfer, with reorganization of the bonding mode of the C_7 ring. On the other hand, chemical and electrochemical tests agree that the oxidation **3** → **2** is a complicated, irreversible, process.

(14) See supplementary Figure 7s.

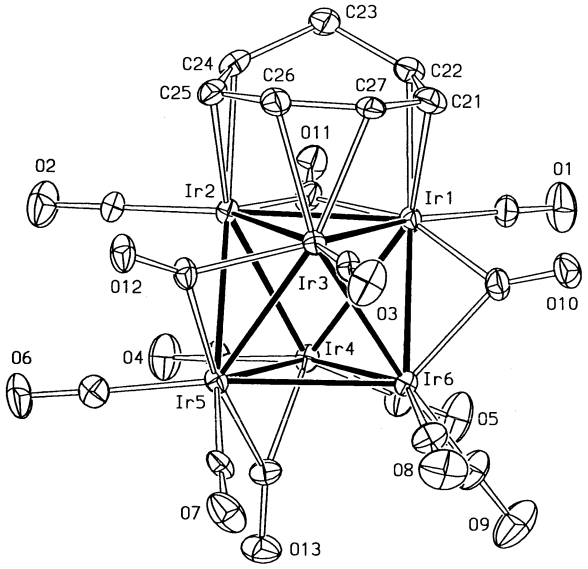

Figure 2. Solid state structure of $[Ir_6(CO)_{13}(C_7H_8)]$. Ellipsoids are drawn at the 30% probability level. The carbon atoms of the carbonyls are labeled as the oxygen to which they are attached.

All the electron transfer mechanisms can be summarized in the following scheme, more straightforward than the paths described in the previous section; differences between chemical and electrochemical process were expected, considering that the former are initiated by acid−base reactions and the latter by outer sphere electron transfers.

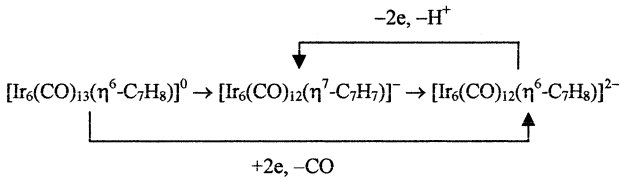

We would like to conclude by paying some attention to the oxidation peak B ($E_p = +0.93$ V, at 0.2 V s^{-1}), which is present in the voltammetric profiles of both **1** and **3**. On the basis of the relative peak heights of the processes illustrated in Figure 1a, it seems reliable to assume that also such an anodic process involves a two-electron transfer. Since cycloheptatriene undergoes a two-electron oxidation to the tropylium ion $[C_7H_7]^+$,[15] such an anodic step might arise from the oxidation of the peripheral C_7H_8 ligand. As a matter of fact, however, under the present experimental conditions, free cycloheptatriene undergoes an irreversible oxidation at $E_p = +1.53$ V (at 0.2 V s^{-1}), and $Cr(CO)_3(\eta^6\text{-}C_7H_8)$ undergoes a first irreversible oxidation at $E_p = +0.64$ V (at 0.2 V s^{-1}), which by comparison with $Cr(CO)_3(\eta^6\text{-}C_6H_6)$ is assigned to the $Cr^{0/+1}$ oxidation,[16] followed by a further irreversible oxidation at $E_p = +1.54$ V (at 0.2 V

(15) Geske, D. H. *J. Am. Chem. Soc.* **1959**, *81*, 4145.
(16) Zoski, C. G.; Sweigart, D. A.; Stone, N. J.; Rieger, P. H.; Mocellin, E.; Mann, T. F.; Mann, D. R.; Gosser, D. K.; Doeff, M. M.; Bond, A. M. *J. Am. Chem. Soc.* **1988**, *110*, 2109.

Table 1. Selected Interatomic Distances (Å) and Angles (deg) for Clusters 1, 2, and 3 with Estimated Standard Deviations (esd's) in Parentheses

	$[Ir_6(CO)_{13}(C_7H_8)]$	$[Ir_6(CO)_{12}(C_7H_7)]^-$	$[Ir_6(CO)_{12}(C_7H_8)]^{2-}$		$[Ir_6(CO)_{13}(C_7H_8)]$	$[Ir_6(CO)_{12}(C_7H_7)]^-$	$[Ir_6(CO)_{12}(C_7H_8)]^{2-}$
Ir1−Ir2	2.729(1)	2.835(1)	2.775(1)	Ir3−C12	1.994(7)	2.035(7)	2.016(9)
Ir1−Ir3	2.819(1)	2.796(1)	2.764(1)	Ir4−C11		2.056(9)	1.997(9)
Ir1−Ir4	2.815(1)	2.787(1)		Ir4−C13	2.050(7)		
Ir1−Ir5			2.785(1)	Ir5−C12	2.157(7)	2.017(8)	2.012(11)
Ir1−Ir6	2.755(1)	2.719(1)	2.693(1)	Ir5−C13	2.115(7)		
Ir2−Ir3	2.750(1)	2.757(1)	2.798(1)	Ir6−C10	2.025(7)	1.959(7)	2.051(9)
Ir2−Ir4	2.738(1)	2.719(1)	2.741(1)	Ir1−C21	2.233(8)	2.299(7)	2.223(10)
Ir2−Ir5	2.853(1)	2.765(1)		Ir1−C22	2.231(8)	2.197(7)	2.148(10)
Ir2−Ir6			2.730(1)	Ir1−C23		2.346(8)	
Ir3−Ir4			2.757(1)	Ir2−C24	2.211(7)	2.190(6)	2.203(10)
Ir3−Ir5	2.759(1)	2.710(1)	2.722(1)	Ir2−C25	2.251(7)	2.226(7)	2.260(10)
Ir3−Ir6	2.769(1)	2.783(1)		Ir3−C26	2.183(7)	2.221(8)	2.193(7)
Ir4−Ir5	2.774(1)	2.801(1)	2.777(1)	Ir3−C27	2.189(7)	2.211(6)	2.206(9)
Ir4−Ir6	2.794(1)	2.778(1)	2.810(1)	C21−C22	1.35(1)	1.39(1)	1.38(2)
Ir5−Ir6	2.822(1)	2.794(1)	2.811(1)	C22−C23	1.52(1)	1.42(1)	1.50(2)
Ir1−C1	1.910(7)	1.882(8)	1.845(8)	C23−C24	1.53(1)	1.41(1)	1.47(1)
Ir2−C2	1.858(8)	1.849(9)	1.822(10)	C24−C25	1.40(1)	1.43(1)	1.46(2)
Ir3−C3	1.902(7)	1.852(9)	1.842(10)	C25−C26	1.47(1)	1.46(1)	1.47(2)
Ir4−C4	1.875(7)	1.864(8)	1.843(12)	C26−C27	1.43(1)	1.44(1)	1.41(1)
Ir4−C5	1.908(8)	1.866(7)	1.868(11)	C27−C21	1.45(1)	1.47(1)	1.49(1)
Ir5−C6	1.896(7)	1.880(8)	1.859(9)	C22−C21−C27	127.6(7)	130.4(9)	130.3(9)
Ir5−C7	1.909(7)	1.869(9)	1.853(11)	C21−C22−C23	126.4(7)	123.6(7)	122.7(9)
Ir6−C8	1.902(9)	1.866(9)	1.847(12)	C22−C23−C24	117.8(7)	130.0(8)	119.8(1.0)
Ir6−C9	1.862(8)	1.879(9)	1.840(9)	C23−C24−C25	125.6(7)	126.4(8)	126.6(1.1)
Ir1−C10	2.085(8)	2.130(10)	1.984(11)	C24−C25−C26	125.5(7)	130.5(7)	124.1(8)
Ir1−C11	2.233(8)			C25−C26−C27	128.6(7)	125.3(7)	130.3(1.0)
Ir2−C11	2.021(7)	2.042(8)	2.038(9)	C26−C27−C21	128.4(7)	127.5(8)	126.3(1.1)

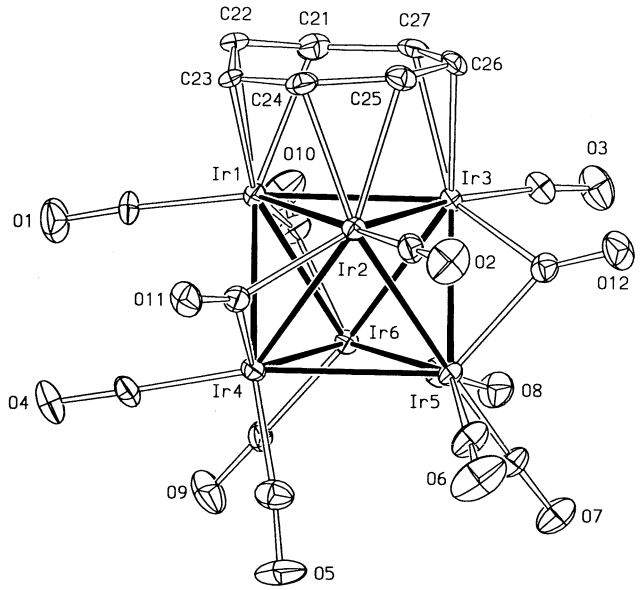

Figure 3. Solid state structure of $[Ir_6(CO)_{12}(C_7H_7)]^-$. Other details as in Figure 1.

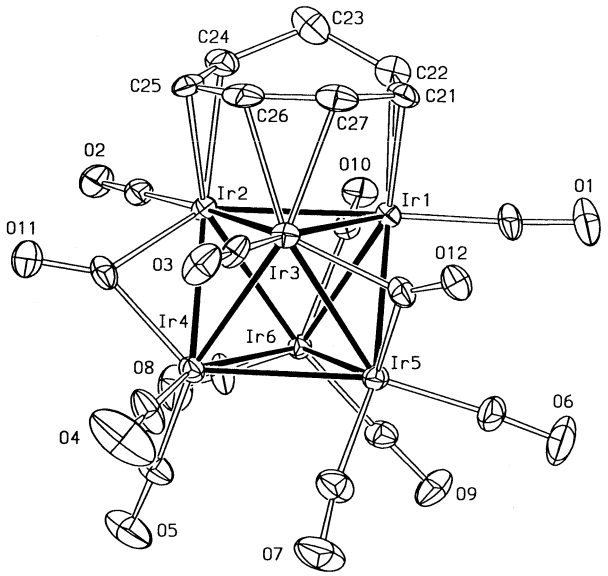

Figure 4. Solid state structure of $[Ir_6(CO)_{12}(C_7H_8)]^{2-}$. Other details as in Figure 1.

s^{-1}) intuitively assigned to the ligand oxidation. In view of the notable differences in redox potentials, to account for the possibility that peak B might involve a ligand-centered process, one must assume that the Ir_6 core exerts a strong electron-donating effect toward the cycloheptatriene ligand. On the other hand, $[Ir_6(CO)_{12}(\eta^7\text{-}C_7H_7)]^-$, which lacks the intact C_7H_8 ligand, does not exhibit the oxidation process under subject.

(3) Solid State Structures. The solid state structures of the clusters **1**, **2**, and **3** are shown in Figures 2, 3, and 4, respectively; important structural parameters are collected in Table 1. Common features are the octahedral metal cages and the presence of the organic ring, sitting on top of one triangular face; for clarity, the atoms composing this face were always numbered Ir1, Ir2, and Ir3. These three metal vertexes are always coordinated by one terminal CO, and the other three

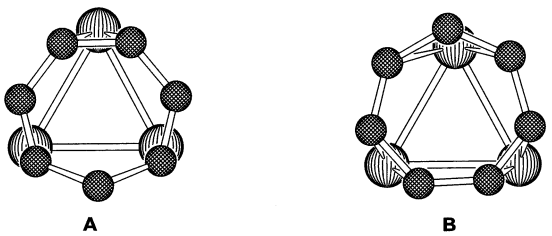

Figure 5. Relative orientation of the C_7 ring and the iridium atoms to which it is bound in (A) **1** and (B) **2**.

by two terminal carbonyl ligands. Figure 5 shows the relative orientation of the organic cyclic ligand and the triangular iridium faces in **1** (which is also representative of the situation found in **3**) and **2**.

(3a) $[Ir_6(CO)_{13}(C_7H_8)]$. The solid state structure of this cluster was determined on a crystal of **1**·$PhCH_3$.

Table 2. Average Bond Lengths (in Å) and Angles (deg) in 1, 2, and 3

	$[Ir_6(CO)_{13}(C_7H_8)]$	$[Ir_6(CO)_{12}(C_7H_7)]^-$	$[Ir_6(CO)_{12}(C_7H_8)]^{2-}$
Ir−Ir	2.781	2.770	2.763
Ir−CO (term)	1.891	1.867	1.847
Ir−CO (bridg)	2.077	2.040	2.016
C−O (term)	1.13	1.15	1.15
C−O (bridg)	1.16	1.17	1.20
Ir−C (ring)	2.216	2.241	2.206
C−C, multiple bonds	1.42	1.43	1.44
Ir−C−O(term)	177.8	177.0	176.5

In the neutral derivative **1** four edge-bridging carbonyl ligands are arranged around two opposite vertexes, spanning two mutually perpendicular pairs of metal−metal bonds This distribution is reminiscent of that found in the black isomer of $Ir_6(CO)_{16}$.[17] The six π electrons of the ligand are involved in a η^2:η^2:η^2 interaction, donating two electrons to each iridium atom, whereas the CH_2 group is bent outward. The C−C bond lengths are scattered in the range 1.35−1.53 Å and are consistent with a localized description of the C−C bonds: the three double bonds involved in the metal−ligand coordination are short; the "truly" simple C−CH_2 bonds are long.

(3b) $[Ir_6(CO)_{12}(C_7H_7)]^-$. The X-ray analysis was performed on two different crystals, $[NEt_4]$**2**·THF and $[NEt_4]$**2**·CH_2Cl_2. The geometry of the anion was very similar in the two compounds, but the data for the second collection were of much higher quality and are here reported. In the monoanion **2** the bridging CO connects three couples of iridium atom, a situation that recalls that found in the dianion $[Ir_6(CO)_{15}]^{2-}$.[18] The cycloheptatrienyl ring is almost planar, with puckering of less than 0.2 Å. Its π-electron system is involved in one allylic and two olefinic interactions (the η^3:η^2:η^2 coordination type). In other clusters, one carbon atom, shared by two allylic systems, is found at bonding distances from two metal atoms; the hapticity of the ligand in this situation is described as η^3:η^3:η^2. However, the two limiting arrangements are not very different. The matching of a heptagon with a triangle is a difficult task,[10] and the result is the best compromise between C−metal bond optimization, ring deformation, sterical interactions with the carbonyls, and solid state packing.[4] As a result, the hapticity of the C_7H_7 rings in $[Co_4(CO)_6(C_7H_9)(C_7H_7)]$ and $[Ru_6C(CO)$-$(C_7H_9)(C_7H_7)]$ appears very similar, but was described in two different ways.[3,4]

In the present case, we think that there is no ambiguity, since C21 and C23 (the two external C atoms of the allyl system) are very far from the nonbonded iridium atoms (close-contact distances >2.8 Å). The Ir1−C21 and Ir1−C23 distances (2.300(7) and 2.346(8) Å, respectively) are rather long and may reflect a low Ir−C bond order, needed to reduce the excess of electrons accumulating on Ir1. However, formally correct distributions of electrons and ligand result if this anion is conceived as a derivative of $[Ir_6(CO)_{15}]^{2-}$, substituted by a tropylium cation.

(3c) $[Ir_6(CO)_{12}(C_7H_8)]^{2-}$. In the dianion **3**, the disposition of the bridging carbonyls is identical to that found in **2**, with three edge-bridging, and the cycloheptatriene is bound in an η^2:η^2:η^2 fashion, as in **1**. Therefore, in this cluster the formal distribution of electrons over the six iridium atoms is optimized.

Scheme 1. Numbering Scheme of the Hydrogen Atoms of the Cycloheptatriene Ring

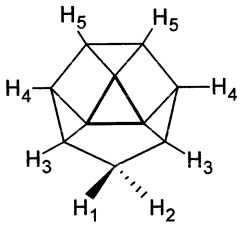

The average bond lengths for the three clusters can be compared in Table 2. Although the differences are small and sometimes comparable with the estimated standard deviation, constant trends are evident and consistent with an increased back-donation of a higher negative charge, to be distributed over a lower number of ligands. As a matter of fact, in the sequence **1**−**2**−**3** the Ir−Ir and the Ir−ligand (both carbonyl and organic ring) bond shorten, whereas the C−O distance increases. The metal−metal distances of the two triangular faces Ir1−Ir2−Ir3 (which carries the C_7 ring) and Ir4−Ir5−Ir6 (parallel to it) are always very similar, suggesting that the metallic framework must not be stretched to optimize the Ir−C interaction, no matter which is the actual coordination of the ring. Of course, a comparison of the C−C average bond length is of little meaning, because of the larger standard deviations and the different bond orders in the two arrangements.

(4) Spectroscopy. (4a) ^{1}H NMR Spectra. The spectra of **1** and **3** are similar and can be discussed together, referring to the numbering of Scheme 1. For the spectrum of $[Ir_6(CO)_{13}(C_7H_8)]$, a few crystals of **1**·PhMe were dissolved in $CDCl_3$. Five multiplets, corresponding to the five nonequivalent protons of the ligand, were present at δ = 2.91(dt, H_1), 4.09(t, H_3), 4.26(m, H_4), 4.48(d, H_2), and 5.12(m, H_5). The signals for the methylenic protons could be easily assigned, on the basis of their intensity, and the geminal coupling constant $^2J(H_1-H_2)$ = 16 Hz. The multiplet at higher field is attributed to the hydrogen that points inward and is more shielded by the metals; the vicinal $^3J(H_1-H_3) = 6$ Hz was also measured. The three remaining signals, due to the vinylic protons, have been assigned with a bidimensional COSY experiment. The signals of toluene, at δ = 2.38 and 7.23, are also present, and their intensity is in agreement with the formula of the compound.

The assignments for $[Ir_6(CO)_{12}(C_7H_8)]^{2-}$ were obtained similarly. The spectrum of $[PPh_4]_2$**2** was recorded in acetone-d_6; its five signals appear at δ = 2.84(dt, H_1),

(17) Garlaschelli, L.; Martinengo, S.; Bellon, P. L.; Demartin, F.; Manassero, M.; Chiang, M. Y.; Bau, R. *J. Am. Chem. Soc.* **1984**, *106*, 6664.

(18) Demartin, F.; Manassero, M.; Sansoni, M.; Garlaschelli, L.; Martinengo, S. *J. Chem. Soc., Chem. Commun.* **1980**, 903.

Table 3. Crystallographic Data

	1·C_6H_5Me	$[N(C_2H_5)_4]$**2**·CH_2Cl_2	$[NMe_3CH_2Ph]_2$**3**
formula	$C_{27}H_{16}Ir_6O_{13}$	$C_{28}H_{29}Cl_2Ir_6NO_{12}$	$C_{39}H_{40}Ir_6N_2O_{12}$
M	1701.62	1795.65	1882.00
color	black	black	black
cryst syst	monoclinic	triclinic	triclinic
space group	$P2_1/n$ (no.14)	$P\bar{1}$ (no.2)	$P\bar{1}$ (no.2)
a/Å	10.469(1)	10.108(1)	11.146(1)
b/Å	20.188(2)	11.736(1)	12.358(1)
c/Å	15.003(2)	16.974(2)	16.214(2)
α/deg	90	109.86(1)	75.63(1)
β/deg	96.33(1)	101.40(1)	86.55(1)
γ/deg	90	95.30(1)	75.54(1)
U/Å^3	3151.5(6)	1828.5(4)	2094.9(4)
Z	4	2	2
F(000)	2976	1592	1692
D_c/g cm^{-3}	3.586	3.261	2.983
T/K	223	223	223
cryst dimens/mm)	0.20 × 0.23 × 0.39	0.17 × 0.28 × 0.28	0.11 × 0.39 × 0.50
μ (Mo Kα)/cm^{-1}	252.1	218.8	189.8
min. and max. transmn factors	0.48−1.00	0.51−1.00	0.25−1.00
scan mode	*ω*	*ω*	*ω*
frame width/deg	0.30	0.30	0.30
time per frame/s	25	25	25
no. of frames	2450	2450	2450
detector−sample distance/cm	5.00	5.00	5.00
θ-range/deg	3−26	3−26	3−26
reciprocal space explored	full sphere	full sphere	full sphere
no. of reflns (total; ind)	40 361; 8142	22 936; 9035	25 821; 10 214
R_{int}	0.067	0.047	0.092
final R_2 and R_{2w} indices[a] (F^2, all reflns)	0.045, 0.059	0.054, 0.074	0.068, 0.090
(conventional R_1 index $I > 2\sigma(I)$)	0.025	0.031	0.039
no. of reflns with $I > 2\sigma(I)$	5681	6834	6820
no. of variables	381	442	532
goodness of fit[b]	0.99	0.99	1.00

[a] $R_2 = [\sum(|F_o^2 - kF_c^2|)/\sum F_o^2]$, $R_{2w} = [\sum w(F_o^2 - kF_c^2)^2/\sum w(F_o^2)^2]^{1/2}$. [b] $[\sum w(F_o^2 - kF_c^2)^2/(N_o - N_v)]^{1/2}$, where $w = 4F_o^2/\sigma(F_o^2)^2$, $\sigma(F_o^2) = [\sigma^2(F_o^2) + (0.04F_o^2)^2]^{1/2}$, N_o is the number of observations and N_v the number of variables.

3.20(t, H_3), 3.64(m, H_4), 4.56(m, H_5), and 4.68(d, H_2). The coupling constants for H_1 are $^2J(H_1-H_2) = 15$ and $^3J(H_1-H_3) = 6$ Hz.

The spectrum for $[NEt_4][Ir_6(CO)_{12}(C_7H_7)]$ in thf-d_8 is much more simple, consisting of a sharp singlet at $\delta = 4.28$, both at room temperature and at 183 K. This singlet confirms that the ligand is fluxional even at low temperature. This behavior is typical for a planar cycloheptatrienylic ligand and averages its donating power to the three coordinated metal centers.[10]

(4b) IR Spectra. The IR absorptions of **1**, **2**, and **3**, in the zone of the carbonyl stretching, are listed in the Experimental Section.[19] Apart from a shift to lower wavenumbers, on increasing the anionic charge, the three spectra have similar patterns in the zone of the terminal ligands: five bands are present, and the peripheral are always less intense. This analogy is not surprising, since the three compounds have the same disposition of terminal carbonyl ligands.

Experimental Section

All the solvents were purified and dried by conventional methods and stored under nitrogen. All the reactions were carried out under oxygen-free nitrogen atmospheres using the Schlenk-tube technique.[20] $[Ir_6(CO)_{16}]$[17] was prepared by literature methods. Infrared spectra in solution were recorded on a Perkin-Elmer 16 PC FT-IR spectrophotometer, using calcium fluoride cells previously purged with N_2. Elemental analyses were carried out by the staff of Laboratorio di Analisi of the Dipartimento di Chimica Inorganica, Metallorganica e Analitica. ^{1}H NMR spectra were recorded on a Bruker 300 spectrometer.

Materials and apparatus for electrochemistry have been described elsewhere.[21] All the potential values are referred to the Saturated Calomel Electrode (SCE). Under the present experimental conditions the one-electron oxidation of ferrocene occurs at $E^{o\prime} = +0.38$ V. Hydrodynamic voltammetry (direct current voltammetry at a platinum electrode with periodical renewal of the diffusion layer) was carried out as previously described.[22] $Cr(CO)_3(\eta^6\text{-}C_7H_8)$ was an Aldrich product.

Synthesis of $[Ir_6(CO)_{13}(C_7H_8)]$ (1). $[Ir_6(CO_{16}]$ (0.43 g; 0.27 mmol) and cycloheptatriene (0.4 mL, 4 mmol) were suspended in 12 mL of toluene. The mixture was refluxed for 7 h, and the resulting dark brown solution was allowed to cool overnight to room temperature. The crystalline precipitate was collected by filtration, washed with hexane, and used for chemical characterization. Yield: 0.28 g; 65%. A second crop can be obtained from the solution by drying in a vacuum the solvent and washing the residue with hexane (3 × 5 mL). Anal. Calcd for $C_{20}H_8Ir_6O_{13}$: C, 14.92; H, 0.50. Found: C, 14.7; H, 0.5. On freshly isolated samples, the content of C and H is higher, owing to the presence of cocrystallized toluene. *ν*(CO) in THF solution: 2093s, 2064vs, 2054sh, 2028s, 2003m, 1982w, 1819m, 1777w cm^{-1}.

Synthesis of $NEt_4[Ir_6(CO)_{12}(C_7H_7)]$ (2). $[Ir_6(CO_{13}(C_7H_8)]$ (0.23 g; 0.14 mmol) and Na_2CO_3 (0.23 g, 2.1 mmol) were suspended in 12 mL of THF and stirred vigorously for 6 h.

(19) See supplementary Figure 6s.

(20) Shriver D. F.; Dredzon, M. A. *The Manipulation of Air-Sensitive Compounds*, 2nd ed.; Wiley: New York, 1986.

(21) Bianchini, C.; Meli, A.; Laschi, F.; Vacca, A.; Zanello, P. *J. Am. Chem. Soc.* **1988**, *110*, 3913.

(22) Ceriotti, A.; Della Pergola, R.; Garlaschelli, L.; Laschi, F.; Manassero, M.; Masciocchi, N.; Sansoni, M.; Zanello, P. *Inorg. Chem.* **1991**, *30*, 3349.

The dark solution was filtered to eliminate the excess of carbonate and dried in a vacuum. The black residue was dissolved in methanol (10 mL). Solid NEt_4Br (0.5 g) was added, and the product was precipitated by addition of water (20 mL). The dark solid was collected by filtration, washed with water, and dried. Crystals were obtained by dissolving the crude product in the minimum amount of CH_2Cl_2 or THF and layering the solution with cyclohexane. Yield: 0.14 g; 57%. Anal. Calcd for $C_{27}H_{27}Ir_6NO_{12}\cdot C_4H_8O$: C, 20.88; H, 1.98; N, 0.79. Found: C, 20.8; H, 1.8; N, 0.8. On aged samples, the content of C and H is lower, due to the loss of cocrystallized THF. ν(CO) in THF solution: 2056w, 2040m, 2022m, 1997vs, 1965m, 1784m cm^{-1}.

Synthesis of $(NEt_4)_2[Ir_6(CO)_{12}(C_7H_8)]$ (3). The product was usually obtained in a one-pot synthesis. In a typical preparation $[Ir_6(CO)_{16}]$ (0.90 g; 0.6 mmol) and cycloheptatriene (0.9 mL, 8 mmol) were suspended in toluene and refluxed for 6 h. The still hot solution was filtered, and the solvent eliminated in a vacuum. Unreacted C_7H_8 was extracted with hexane, and crude **1** was dissolved in 10 mL of THF. A solution of NaOH in MeOH (2 M, 2 mL) was added, and the mixture was stirred for 2 h. The solvent was dried in a vacuum, and the sodium salt Na_2**3** was dissolved in MeOH (5 mL). Solid $[NMe_3CH_2Ph]Cl$ was added, and the resulting precipitate was collected by filtration, washed with 2-propanol, and dried. Crystals were obtained by dissolving the crude product in the minimum amount of acetone and layering the solution with 2-propanol. Yield: 27%. Anal. Calcd for $C_{27}H_{27}Ir_6NO_{12}$: C, 24.89; H, 2.14; N, 1.49. Found: C, 24.9; H, 2.3; N, 1.3. ν(CO) in acetonitrile solution: 2010m, 1964vs, 1937m, 1739m cm^{-1}.

X-ray Data Collections and Structure Determinations. Crystal data and other experimental details are summarized in Table 3. The diffraction experiments were carried out on a Bruker SMART CCD area-detector diffractometer at 223 K using Mo Kα radiation ($\lambda = 0.71073$ Å) with a graphite crystal monochromator in the incident beam. Cell parameters and orientation matrixes were obtained from the least-squares refinement of 114 (for **1**$\cdot C_6H_5Me$), 71 (for $[N(C_2H_5)_4]$**2**$\cdot CH_2Cl_2$), and 89 (for $[NMe_3CH_2Ph]_2$**3**) reflections measured in three different sets of 15 frames each, in the range $3° < \theta < 23°$. At the end of data collections the first 50 frames, containing 405, 243, and 232 reflections (for **1**$\cdot C_6H_5Me$, $[N(C_2H_5)_4]$**2**$\cdot CH_2Cl_2$, and $[NMe_3CH_2Ph]_2$**3**, respectively), were recollected to have a monitoring of crystal decay, which was not observed, so that no time-decay correction was needed. The collected frames were processed with the software SAINT,[23] and an empirical absorption correction was applied (SADABS)[24] to the collected reflections. Scattering factors and anomalous dispersion corrections were taken from ref 25. The calculations were performed on a Pentium III PC using the Personal Structure Determination Package[26] and the physical constants tabulated therein. The structures were solved by direct methods (SHELXS 86)[27] and refined by full-matrix least-squares, using all reflections and minimizing the function $\sum w(F_o^2 - k|F_c|^2)^2$ (refinement on F^2). Anisotropic thermal factors were refined for all the nonhydrogen atoms, with the exception of the carbon atoms of the toluene molecule in **1**$\cdot C_6H_5Me$, which were refined isotropically. The hydrogen atoms of the toluene methyl group in **1**$\cdot C_6H_5Me$ were neglected. All the other hydrogen atoms were placed in their ideal positions (C−H = 0.97 Å, B 1.10 times that of the carbon atom to which they are attached) and not refined. The final Fourier maps show maximum residuals of 1.9(4) e/Å^3 at 0.99 Å from Ir(3) for **1**$\cdot C_6H_5Me$, 2.3(6) e/Å^3 at 0.87 Å from Ir(3) for $[N(C_2H_5)_4]$**2**$\cdot CH_2Cl_2$, and 4.2(9) e/Å^3 at 0.96 Å from Ir(1) for $[NMe_3CH_2Ph]_2$**3**.

The atomic coordinates of the structure models have been deposited with the Cambridge Crystallographic Data Center.

Acknowledgment. This work was funded by MURST (Cofin 2000 and ex 60%).

Supporting Information Available: Tables of atomic coordinates, anisotropic thermal parameters (U's) for the nonhydrogen atoms, full list of bond distances and angles for **1**, **2**, and **3**. Figure 6s: IR spectra of (a) **1** in THF, (b) $[NEt_4]$**2** in THF, and (c) $[PPh_4]_2$**3**, in MeCN. Figure 7s: Cyclic voltammograms recorded at a platinum electrode during the progressive coulometric oxidation of a MeCN solution of $[Ir_6(CO)_{12}(\eta^6\text{-}C_7H_8)]^{2-}$ (2.0×10^{-3} mol dm^{-3}) in correspondence with the first anodic step ($E_w = 0.0$ V). Scan rate 0.2 V s^{-1}. This material is available free of charge via the Internet at http://pubs.acs.org.

OM0204437

(23) *SAINT*, Reference manual; Siemens Energy and Automation; Madison, WI, 1994−1996.
(24) Sheldrick, G. M. *SADABS*, Empirical Absorption Correction Program; University of Gottingen, 1997.
(25) *International Tables for X-ray Crystallography*; Kynoch Press: Birmingham, 1974; Vol. 4.
(26) Frenz, B. A. (a) *Comput. Phys.* **1988**, *2*, 42. (b) *Crystallographic Computing 5*, Oxford University Press: Oxford, UK, 1991; Chapter 11, p 126.
(27) Sheldrick, G. M. *SHELXS86*, program for the solution of crystal structures; University of Gottingen: Federal Republic of Germany, 1985.